FUDMA Journal of Sciences (FJS)
ISSN online: 2616-1370
ISSN print: 2645 - 2944
Vol. 10 No. 13, July, 2026, pp 21 – 26
DOI: https://doi.org/10.33003/fjs-2026-1013-5684

Predictive Finite-Time Multi-Switching Synchronisation of Fractional-Order Hyperchaotic Systems for Seismic Signal Analysis and Earthquake Stability Monitoring

[1]Makarios A. Emmanuel, *[2]Adamu Z. Ngari, [2]Oyono S. Job, [3]Jamilu M. Garba, [1]Yakubu H. Ngadda and [4]Olasunkanmi I. Olusola

[1]Department of Physics, University of Maiduguri, Maiduguri, Nigeria.
[2]Department of Physics, Nigerian Army University Biu. Borno State.
[3]Department of Science Laboratory Technology, Nigerian Building and Research Institute, Kano State.
[4]Department of Physics, Lagos State University.

*Corresponding authors' email: adamuzngari886@gmail.com

ABSTRACT
Earthquake systems are highly nonlinear, memory-dependent and characterised by hidden instability, making conventional deterministic and statistical monitoring approaches inadequate for capturing irregular seismic behaviour. This study proposes an Predictive finite-time multi-switching synchronisation framework for fractional-order hyperchaotic systems applied to seismic signal analysis and earthquake stability monitoring. The framework combines memristive, hidden-attractor and neural hyperchaotic dynamics within a multi-drive multi-response architecture to represent memory effects, concealed instability and adaptive nonlinear signal behaviour. The Caputo fractional derivative is employed to model hereditary geophysical characteristics associated with tectonic loading, stress accumulation and delayed crustal response. Multi-switching synchronisation errors are formulated explicitly, and adaptive finite-time controllers are designed to guarantee rapid convergence despite nonlinear uncertainty and parameter variation. Lyapunov stability theory is used to establish sufficient conditions for finite-time convergence of the synchronisation errors. Numerical implementation is carried out in MATLAB, where phase portraits, time-series responses, synchronisation error trajectories, error norms, drive-response tracking and bifurcation behaviour are analysed. The simulation results indicate that the proposed method achieves stable and rapid synchronisation, while preserving the complex nonlinear features required for realistic seismic modelling. The framework also demonstrates potential for identifying abnormal transitions, interpreting hidden fault activation and monitoring changes in earthquake-related dynamical stability. Overall, the study provides a unified nonlinear modelling and control approach that integrates fractional calculus, hyperchaos and adaptive synchronisation for improved seismic anomaly detection and earthquake stability assessment. It further establishes a computational foundation for future validation using recorded seismic datasets, real-time monitoring platforms and experimentally calibrated geophysical parameter values in practice.

Received: 2 Jul. 2026

Accepted: 16 Jul. 2026

Published: 3 Aug 2026

Keywords: Fractional-Order Systems, Hyperchaotic Systems, Adaptive Finite-Time Synchronisation, Seismic Signal Analysis, Earthquake Stability Monitoring, Hidden Attractors, Memristive Systems, Nonlinear Geophysics

INTRODUCTION

Earthquake systems are among the most complex geophysical phenomena because they involve nonlinear interaction among tectonic stress accumulation, crustal deformation, fault rupture and seismic wave propagation. Despite advances in seismology and computational geophysics, reliable earthquake stability monitoring remains difficult because seismic systems often exhibit uncertainty, multiscale behaviour and hidden instability (Geller et al., 1997; Turcotte, 2002; Scholz, 2019).

Traditional seismic signal analysis methods have contributed significantly to earthquake interpretation; however, many of them rely on deterministic, statistical or linearised assumptions. Such approaches may be insufficient for representing nonlinear transitions, concealed fault activation and irregular precursor signals. Recent computational seismology has therefore encouraged nonlinear and intelligent approaches for analysing seismic signals and detecting hidden geophysical anomalies (Bergen et al., 2019; Mousavi and Beroza, 2022).

Chaos and hyperchaos theory provide mathematical tools for modelling deterministic systems that exhibit irregular and unpredictable behaviour. Hyperchaotic systems are especially useful because they possess more than one positive Lyapunov exponent and are capable of generating richer nonlinear dynamics than ordinary chaotic systems (Lorenz, 1963; Pecora and Carroll, 1990; Petra´sˇ, 2011). These features make hyperchaotic systems suitable for modelling complex earthquake dynamics, where small changes in fault conditions may result in largescale seismic consequences.

The debate on earthquake precursors further shows the need for nonlinear and data-driven monitoring frameworks capable of distinguishing genuine geophysical instability from uncertain precursor claims (De Santis et al., 2019).

Fractional-order systems extend classical integer-order models by incorporating memory and hereditary effects. This is important in geophysical modelling because present fault

behaviour may depend on previous tectonic loading, accumulated stress and delayed crustal response. The Caputo fractional derivative is particularly suitable for physical applications because it permits conventional initial conditions and supports numerical implementation through predictor-corrector schemes (Podlubny, 1999; Diethelm et al., 2002; Baleanu et al., 2012; Garrappa, 2018).
Memristive systems are useful in nonlinear modelling because they possess memory-dependent properties. In seismic systems, the cumulative effects of previous fault interactions and tectonic loading may influence present geophysical behaviour. Consequently, memristive hyperchaotic systems provide a suitable framework for representing memory-driven seismic dynamics (Chua, 1971; Bao et al., 2021). Hidden-attractor systems are also relevant because their basins of attraction are not connected to unstable equilibrium points, making them suitable for modelling concealed instability and abrupt seismic transitions (Leonov and Kuznetsov, 2013; Dudkowski et al., 2016).
Neural hyperchaotic systems provide an additional advantage for adaptive nonlinear signal interpretation. Seismic precursor signals are often noisy, irregular and difficult to distinguish from background geological fluctuations. Neural nonlinear dynamics can improve adaptive signal representation and support intelligent seismic anomaly analysis (Bergen et al., 2019; Mousavi and Beroza, 2022; Yu et al., 2024).
Synchronisation theory has become an important tool in nonlinear dynamics since the demonstration that chaotic systems can be synchronised under suitable coupling (Pecora and Carroll, 1990). Adaptive finite-time synchronisation improves this process by ensuring convergence within a finite duration rather than merely asymptotically. This is important for earthquake monitoring because seismic instability may evolve rapidly and require prompt detection (Bhat and Bernstein, 2000; Chen et al., 2022; Yu et al., 2024).
Despite these developments, limited attention has been given to the integration of fractional order hyperchaotic systems, hidden attractors, memristive dynamics and neural nonlinear modelling within an adaptive finite-time multi-switching synchronisation framework for earthquake stability monitoring. This paper addresses this gap by proposing a synchronisation-based nonlinear modelling framework for seismic signal analysis and geophysical instability assessment.
The chaotic approach also have a great role in nuclear physics as in the calculation of the binding energy of atomic nuclei. The cumulative mass of these individual nucleons often surpasses the actual mass of the atomic nucleus they create. This disparity in mass, known as the Mass Defect, corresponds to the energy needed to bind the nucleons together against the proton-proton repulsion, as explained by Einstein's mass-energy equivalence (Ngari *et al.,* 2025).

MATERIALS AND METHODS

This study adopts a theoretical, mathematical and simulation-based methodology. The proposed model consists of three fractional-order hyperchaotic drive systems and two response systems. The drive systems represent memory-dependent tectonic loading, hidden seismic instability and adaptive nonlinear signal behaviour, while the response systems are controlled through adaptive finite-time multi-switching synchronisation.

Fractional-Order Representation

The Caputo fractional derivative is adopted as

$$ {}^{C}D_t^q x(t) = \frac{1}{\Gamma(n-q)}\int_0^t \frac{x^{(n)}(\tau)}{(t-\tau)^{q+1-n}}d\tau, \qquad n-1<q<n, \quad (1)$$

where q is the fractional order and Γ is the Gamma function. In this study,

$$0 < q < 1. \quad (2)$$

Drive Systems

The first drive system is the fractional-order memristive hyperchaotic system:

$${}^{C}D_t^q x_1 = a(y_1 - x_1) + w_1 z_1, \quad (3)$$
$${}^{C}D_t^q y_1 = bx_1 - cx_1 z_1 + y_1 + u_1, \quad (4)$$
$${}^{C}D^q_{z1} = x_1 y_1 - dz_1 + v_1, \quad (5)$$
$${}^{C}D^q_{u1} = -k_1 y_1 + r_1 w_1 \quad (6)$$
$${}^{C}D^q_{w1} = -m_1 x_1 + n_1 z_1. \quad (7)$$

The second drive system is the fractional-order hidden-attractor hyperchaotic system:

$${}^{C}D_t^q x_2 = \alpha(y_2 - x_2) + z_2, \quad (8)$$
$${}^{C}D^q_{y2} = \beta x_2 - x_2 z_2 + u_2, \quad (9)$$
$${}^{C}D^q_{z2} = x_2 y_2 - \gamma z_2 + w_2, \quad (10)$$
$${}^{C}D^q_{u2} = -\delta y_2 + \eta w_2, \quad (11)$$
$${}^{C}D^q_{w2} = \mu x_2 - \lambda z_2.$$

The third drive system is the fractional-order neural hyperchaotic system:(2.210)

$${}^{C}D_t^q x_3 = -a_1 x_3 + b_1 \tanh(y_3) + z_3, \quad (12)$$
$${}^{C}D^q_{y3} = -a_2 y_3 + b_2 \tanh(z_3) + u_3, \quad (13)$$
$${}^{C}D^q_{z3} = -a_3 z_3 + b_3 \tanh(x_3) + w_3, \quad (14)$$
$${}^{C}D^q_{u3} = -a_4 u_3 + x_3 y_3, \quad (15)$$
$${}^{C}D^q_{w3} = -a_5 w_3 + y_3 z_3 \quad (16)$$

Response Systems

Let the response systems be

$$R1 = (p1, p2, p3, p4, p5)T \quad (17)$$

and

$$R_2 = (r_1, r_2, r_3, r_4, r_5)^T. \quad (18)$$

The response systems are controlled through adaptive control inputs $U_i(t)$ and $V_i(t)$.

Multi-Switching Error Formulation

The synchronisation errors are defined as

$$e_1 = p_1 - (a_1 x_1 + b_1 y_2 + c_1 z_3), \quad (19)$$
$$e_2 = p_2 - (a_2 y_1 + b_2 z_2 + c_2 u_3), \quad (20)$$
$$e_3 = p_3 - (a_3 z_1 + b_3 u_2 + c_3 w_3), \quad (21)$$
$$e4 = p4 - (a_4 u_1 + b_4 w_2 + c_4 x_3), \quad (22)$$
$$e_5 = p_5 - (a_5 w_1 + b_5 x_2 + c_5 y_3), \quad (23)$$
$$e_6 = r_1 - (d_1 x_1 + d_2 y_2 + d_3 z_3), \quad (24)$$
$$e_7 = r_2 - (d_4 y_1 + d_5 z_2 + d_6 u_3), \quad (25)$$
$$e_8 = r_3 - (d_7 z_1 + d_8 u_2 + d_9 w_3), \quad (26)$$
$$e_9 = r_4 - (d_{10} u_1 + d_{11} w_2 + d_{12} x_3), \quad (27)$$
$$e_{10} = r_5 - (d_{13} w_1 + d_{14} x_2 + d_{15} y_3). \quad (28)$$

The synchronisation objective is

$$\lim_{t\to T_f} \|E(t)\| = 0, \quad (29)$$

Where

$$E(t) = (e_1, e_2, e_3, e_4, e_5, e_6, e_7, e_8, e_9, e_{10})^T. \quad (30)$$

Step-by-Step Derivation of the Error Dynamics and Controller Substitution

The multi-switching synchronisation errors are derived by taking the Caputo fractional derivative of each error variable and substituting the corresponding drive and response system equations. This gives the explicit error dynamics from which the adaptive finite-time controllers are constructed.
For the first error,

$$e_1 = p_1 - (a_1 x_1 + b_1 y_2 + c_1 z_3). \quad (31)$$

Taking the Caputo derivative gives

$${}^{C}D_t^q e_1 = {}^{C}D_t^q p_1 - a_1 {}^{C}D_t^q x_1 - b_1 {}^{C}D_t^q y_2 - c_1 {}^{C}D_t^q z_3. \quad (32)$$

Substituting the system equations,

${}^{C}D^{q}_{e1} = f_1(p) + U_1(t) - a_1[a(y_1 - x_1) + w_1z_1] - b_1[\beta x_2 - x_2z_2 + u_2] - c_1[-a_3z_3 + b_3\tanh(x_3) + w_3].$ (33)
Choose the controller
$U_1(t) = -f_1(p) + a_1[a(y_1 - x_1) + w_1z_1] + b_1[\beta x_2 - x_2z_2 + u_2] + c_1[-a_3z_3 + b_3\tanh(x_3) + w_3] - k_1e_1 - \theta_1\,\mathrm{sgn}(e_1)|e_1|^{\rho}.$
Substituting $U_1(t)$ gives (34)

$${}^{C}D^{q}_{t}e_1 = -k_1e_1 - \theta_1\,\mathrm{sgn}(e_1)|e_1|^{\rho}. \quad (35)$$

For the second error,
$e_2 = p_2 - (a_2y_1 + b_2z_2 + c_2u_3).$ (36)
Taking the Caputo derivative,
${}^{C}D^{q}_{e2} = D^{q}_{p2} - a2\,{}^{C}D^{q}_{y1} - b2\,{}^{C}D^{q}_{z2} - c_2\,{}^{C}D^{q}_{u3}$ (37)

Substitution gives
${}^{C}D^{q}_{e2} = f_2(p) + U_2(t) - a_2[bx_1 - cx_1z_1 + y_1 + u_1] - b_2[x_2y_2 - \gamma z_2 + w_2] - c_2[-a_4u_3 + x_3y_3].$ (38)

Choose
$U_2(t) = -f_2(p) + a_2[bx_1 - cx_1z_1 + y_1 + u_1] + b_2[x_2y_2 - \gamma z_2 + w_2] + c_2[-a_4u_3 + x_3y_3] - k_2e_2 - \theta_2\,\mathrm{sgn}(e_2)|e_2|^{\rho}.$ (39)
Therefore,
$D^{q}_{e2} = -k_2e_2 - \theta_2\,\mathrm{sgn}(e_2)|e_2|^{\rho}.$ (40)
For the third error,
$e_3 = p_3 - (a_3z_1 + b_3u_2 + c_3w_3).$ (41)
Taking the Caputo derivative,
${}^{C}D^{q}_{t}e_3 = {}^{C}D^{q}_{t}p_3 - a_3\,{}^{C}D^{q}_{t}z_1 - b_3\,{}^{C}D^{q}_{t}u_2 - c_3\,{}^{C}D^{q}_{t}w_3.$ (42)
Substitution gives
$D^{q}_{e3} = f_3(p) + U_3(t) - a_3[x_1y_1 - dz_1 + v_1]$ (43)
$- b_3[-\delta y_2 + \eta w_2] - c_3[-a_5w_3 + y_3z_3].$
Choose
$U_3(t) = -f_3(p) + a_3[x_1y_1 - dz_1 + v_1] + b_3[-\delta y_2 + \eta w_2] + c_3[-a_5w_3 + y_3z_3]$
$- k_3e_3 - \theta_3\,\mathrm{sgn}(e_3)|e_3|^{\rho}.$ (44)
Therefore,
${}^{C}D^{q}_{e3} = -k_3e_3 - \theta_3\,\mathrm{sgn}(e_3)|e_3|^{\rho}.$ (45)
For the fourth error,
$e_4 = p_4 - (a_4u_1 + b_4w_2 + c_4x_3).$ (46)
Taking the Caputo derivative,
${}^{C}D^{q}_{t}e_4 = {}^{C}D^{q}_{t}p_4 - a_4\,{}^{C}D^{q}_{t}u_1 - b_4\,{}^{C}D^{q}_{t}w_2 - c_4\,{}^{C}D^{q}_{t}x_3.$ (47)
Substitution gives
${}^{C}D^{q}_{e4} = f_4(p) + U_4(t) - a_4[-k_1y_1 + r_1w_1] - b_4[\mu x_2 - \lambda z_2] - c_4[-a_1x_3 + b_1\tanh(y_3) + z_3].$ (48)
Choose
$U_4(t) = -f_4(p) + a_4[-k_1y_1 + r_1w_1] + b_4[\mu x_2 - \lambda z_2] + c_4[-a_1x_3 + b_1\tanh(y_3) + z_3] - k_4e_4 - \theta_4\,\mathrm{sgn}(e_4)|e_4|^{\rho}.$ (49)
Therefore,
${}^{C}D^{q}_{e4} = -k_4e_4 - \theta_4\,\mathrm{sgn}(e_4)|e_4|^{\rho}.$ (50)
For the fifth error,
$e_5 = p_5 - (a_5w_1 + b_5x_2 + c_5y_3).$ (51)
Taking the Caputo derivative,
${}^{C}D^{q}_{t}e_5 = {}^{C}D^{q}_{t}p_5 - a_5\,{}^{C}D^{q}_{t}w_1 - b_5\,{}^{C}D^{q}_{t}x_2 - c_5\,{}^{C}D^{q}_{t}y_3.$
(52)

Substitution gives
${}^{C}D^{q}_{t}e_5 = f_5(p) + U_5(t) - a_5[-m_1x_1 + n_1z_1]$
$- b_5[\alpha(y_2 - x_2) + z_2] - c_5[-a_2y_3 + b_2\tanh(z_3) + u_3].$ (53)
Choose
$U_5(t) = -f_5(p) + a_5[-m_1x_1 + n_1z_1] + b_5[\alpha(y_2 - x_2) + z_2] + c_5[-a_2y_3 + b_2\tanh(z_3) + u_3] - k_5e_5 - \theta_5\,\mathrm{sgn}(e_5)|e_5|^{\rho}.$ (54)
Therefore,
${}^{C}D^{q}_{e5} = -k_5e_5 - \theta_5\,\mathrm{sgn}(e_5)|e_5|^{\rho}.$ (55)
For the sixth error,
$e_6 = r_1 - (d_1x_1 + d_2y_2 + d_3z_3).$ (56)
Taking the Caputo derivative and substituting,
${}^{C}D^{q}_{t}e_6 = g_1(r) + V_1(t) - d_1[a(y_1 - x_1) + w_1z_1] - d_2[\beta x_2 - x_2z_2 + u_2] - d_3[-a_3z_3 + b_3\tanh(x_3) + w_3].$ (57)
Choose
$V_1(t) = -g_1(r) + d_1[a(y_1 - x_1) + w_1z_1] + d_2[\beta x_2 - x_2z_2 + u_2] + d_3[-a_3z_3 + b_3\tanh(x_3) + w_3] - h_1e_6 - \phi_1\,\mathrm{sgn}(e_6)|e_6|^{\sigma}.$ (58)
Thus,(59)
${}^{C}D^{q}_{t}e_6 = -h_1e_6 - \phi_1\,\mathrm{sgn}(e_6)|e_6|^{\sigma}.$ (60)
For the seventh error,
$e_7 = r_2 - (d_4y_1 + d_5z_2 + d_6u_3).$(61)
Substitution gives
${}^{C}D^{q}_{e7} = g_2(r) + V_2(t) - d_4[bx_1 - cx_1z_1 + y_1 + u_1] - d_5[x_2y_2 - \gamma z_2 + w_2] - d_6[-a_4u_3 + x_3y_3].$(62)
Choose
$V_2(t) = -g_2(r) + d_4[bx_1 - cx_1z_1 + y_1 + u_1] + d_5[x_2y_2 - \gamma z_2 + w_2] + d_6[-a_4u_3 + x_3y_3] - h_2e_7 - \phi_2\,\mathrm{sgn}(e_7)|e_7|^{\sigma}.$ (63)
Thus,
${}^{C}D^{q}_{e7} = -h_2e_7 - \phi_2\,\mathrm{sgn}(e_7)|e_7|^{\sigma}.$ (64)
For the eighth error,
$e_8 = r_3 - (d_7z_1 + d_8u_2 + d_9w_3).$
Substitution gives
${}^{C}D^{q}_{e8} = g_3(r) + V_3(t) - d_7[x_1y_1 - dz_1 + v_1] - d_8[-\delta y_2 + \eta w_2] - {}_9[-a_5w_3 + y_3z_3].$ (65)
Choose
$V_3(t) = -g_3(r) + d_7[x_1y_1 - dz_1 + v_1] + d_8[-\delta y_2 + \eta w_2] + d_9[-a_5w_3 + y_3z_3] - h_3e_8 - \phi_3\,\mathrm{sgn}(e_8)|e_8|^{\sigma}.$ (66)
Thus,
${}^{C}D^{q}_{e8} = -h_3e_8 - \phi_3\,\mathrm{sgn}(e_8)|e_8|^{\sigma}.$ (67)
For the ninth error,
$e_9 = r_4 - (d_{10}u_1 + d_{11}w_2 + d_{12}x_3).$ (68)
Substitution gives
${}^{C}D^{q}_{e9} = g_4(r) + V_4(t) - d_{10}[-k_1y_1 + r_1w_1] - d_{11}[\mu x_2 - \lambda z_2] - d_{12}[-a_1x_3 + b_1\tanh(y_3) + z_3].$ (69)
Choose
$V_4(t) = -g_4(r) + d_{10}[-k_1y_1 + r_1w_1] + d_{11}[\mu x_2 - \lambda z_2] + d_{12}[-a_1x_3 + b_1\tanh(y_3) + z_3] - h_4e_9 - \phi_4\,\mathrm{sgn}(e_9)|e_9|^{\sigma}.$ (70)
Thus
${}^{C}D^{q}_{e9} = -h_4e_9 - \phi_4\,\mathrm{sgn}(e_9)|e_9|^{\sigma}.$ (71)
For the tenth error,
$e_{10} = r_5 - (d_{13}w_1 + d_{14}x_2 + d_{15}y_3).$ (72)
Substitution gives
${}^{C}D^{q}_{t}e_{10} = g_5(r) + V_5(t) - d_{13}[-m_1x_1 + n_1z_1] - d_{14}[\alpha(y_2 - x_2) + z_2] - d_{15}[-a_2y_3 + b_2\tanh(z_3) + u_3].$ (73)
Choose
$V_5(t) = -g_5(r) + d_{13}[-m_1x_1 + n_1z_1] + d_{14}[\alpha(y_2 - x_2) + z_2] + d_{15}[-a_2y_3 + b_2\tanh(z_3) + u_3] - h5e10 - \phi5\,\mathrm{sgn}(e10)|e10|\sigma.$
(74)
Thus,
${}^{C}D^{q}_{t}e_{10} = -h_5e_{10} - \phi_5\,\mathrm{sgn}(e_{10})|e_{10}|^{\sigma}$ (75)
Hence, after controller substitution, all nonlinear terms are cancelled and the complete controlled error system becomes
${}^{C}D^{q}_{ei} = -k_ie_i - \theta_i\,\mathrm{sgn}(e_i)|e_i|^{\rho}, \quad i = 1,2,...,5,$ (76)
and
${}^{C}D^{q}_{ej} = -h_je_j - \phi_j\,\mathrm{sgn}(e_j)|e_j|^{\sigma},$ (77)

Lyapunov Stability Analysis
Consider the Lyapunov candidate function
$j = 6,7,...,10.$ (78)

$$V(t) = \frac{1}{2}\sum_{i=1}^{10} e_i^2. \quad (79)$$

Taking the fractional derivative along the error dynamics gives

$${}^{C}D^{q}_{t}V(t) = \sum_{i=1}^{10} e_i\,{}^{C}D^{q}_{t}e_i. \quad (80)$$

Substituting the controlled error dynamics yields

$${}^{C}D^{q}_{t}V(t) = -\sum_{i=1}^{5} k_ie_i^2 - \sum_{i=1}^{5}\theta_i|e_i|^{\rho+1} - \sum_{j=6}^{10} h_je_j^2 - \sum_{j=6}^{10}\phi_j|e_j|^{\sigma+1}. \quad (81)$$

Since $k_i, h_j, \theta_i, \phi_j > 0$ and $0 < \rho, \sigma < 1$,

$$ {}^{C}D_t^q V(t) < 0, \qquad E(t) \neq 0 \tag{82}$$

Therefore, the synchronisation errors converge to zero within finite time. This proves the stability of the proposed adaptive finite-time multi-switching synchronisation scheme.

Numerical Simulation

The numerical implementation is carried out in MATLAB. Phase portraits, time-series responses, synchronisation error plots, error norms, synchronisation difference and bifurcation diagrams are generated to validate the theoretical results.

RESULT AND DISCUSSION

Phase Portrait Analysis

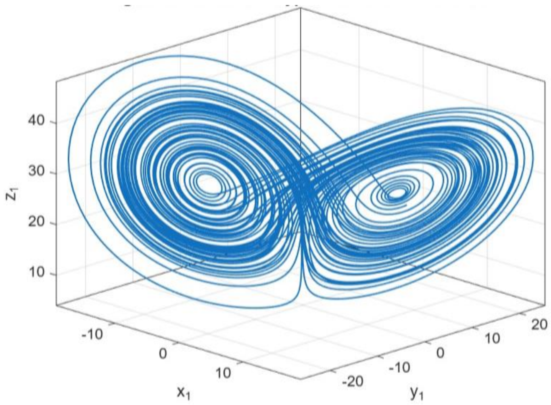

Figure 1: Memristive Hyperchaotic Phase Portrait

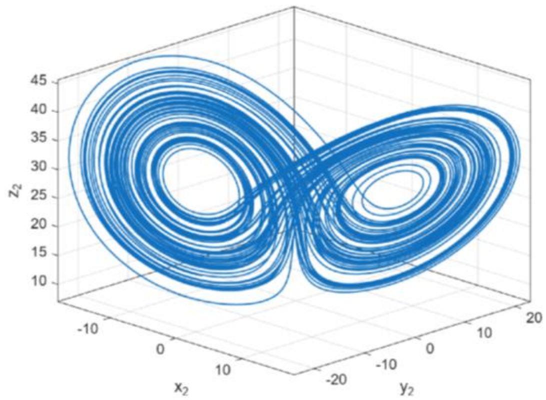

Figure 2: Hidden-Attractor Hyperchaotic Phase Portrait

Figure 1 shows the phase portrait of the memristive hyperchaotic subsystem. The dense doublescroll structure confirms strong nonlinear oscillation and memory-dependent dynamics.

This presents the hidden-attractor subsystem. The observed nonlinear oscillation supports its relevance for concealed fault instability and hidden seismic transition modelling. The neural hyperchaotic subsystem is retained in the analytical framework for adaptive nonlinear signal interpretation. However, its graphical output is excluded from the final discussion because the selected simulation parameters produced numerical divergence

Time-Series Analysis

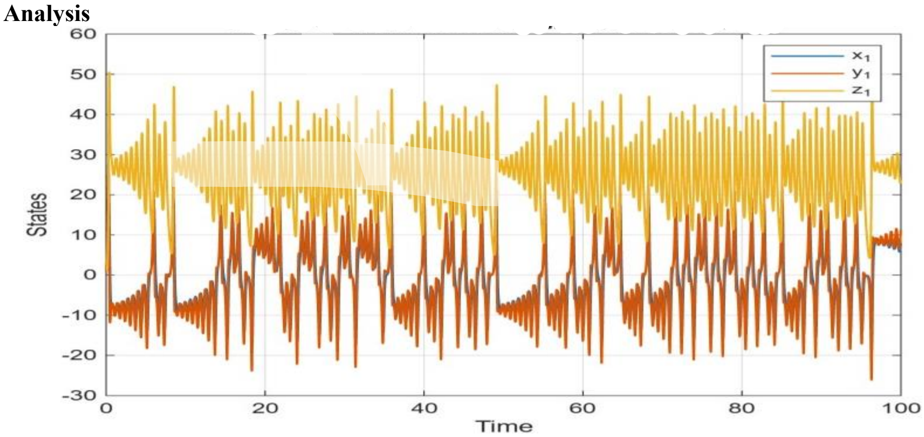

Figure 3: Time-Series Response of the Memristive Hyperchaotic System

Figure 3 shows irregular temporal evolution of the memristive hyperchaotic system. This confirms nonlinear oscillatory behaviour suitable for modelling seismic signal fluctuations.

Synchronisation Error Analysis

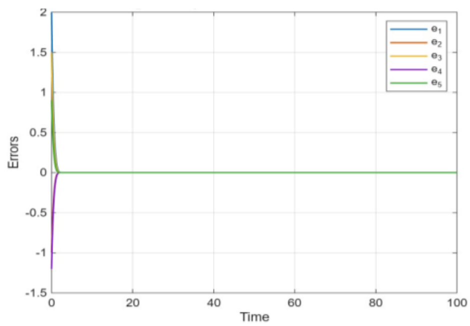

Figure 4: Synchronisation Errors e_1 to e_5.

Figure 4 shows that the first five errors converge rapidly to zero.

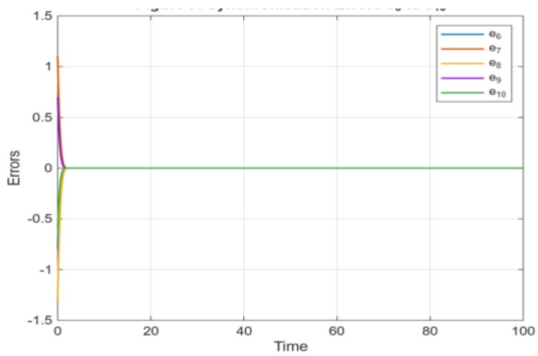

Figure 5: Synchronisation errors e_6 to e_{10}

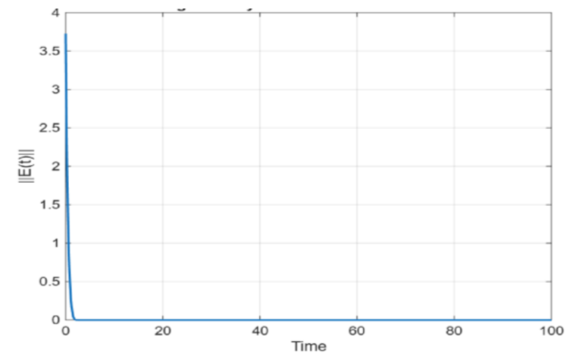

Figure 6: Synchronisation error norm

Figure 5 confirms the convergence of the remaining synchronisation errors.
Figure 6 shows that the total error magnitude approaches zero within finite time.

Synchronisation Difference

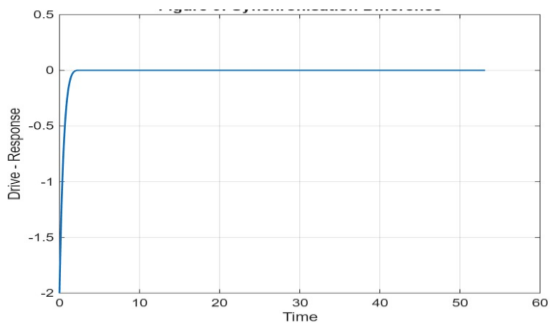

Figure 7: Synchronisation Difference Between Drive and Response Systems

Figure 7 confirms that the difference between the drive and response systems converges to zero.

Bifurcation Analysis

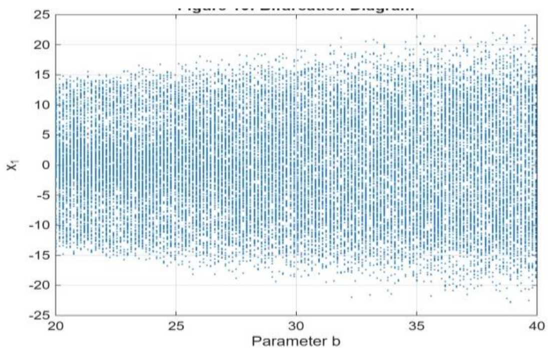

Figure 8: Bifurcation Diagram of the Memristive Hyperchaotic System

Figure 8 shows parameter-sensitive nonlinear behaviour. This supports the suitability of the proposed system for modelling abrupt seismic transitions and nonlinear geophysical instability.
Overall, the results confirm that the proposed adaptive finite-time multi-switching synchronisation framework achieves stable convergence and provides a useful nonlinear structure for seismic signal analysis and earthquake stability monitoring.

CONCLUSION

This paper developed an adaptive finite-time multi-switching synchronisation framework for fractional-order hyperchaotic systems for seismic signal analysis and earthquake stability monitoring. The proposed approach integrated memristive, hidden-attractor and neural hyperchaotic dynamics within a multi-drive multi-response structure. Synchronisation errors were explicitly formulated, adaptive finite-time controllers were designed, and Lyapunov stability analysis confirmed finite-time convergence. MATLAB simulations further demonstrated nonlinear attractor behaviour, rapid error convergence and bifurcation sensitivity. The findings indicate that the proposed framework is suitable for seismic anomaly detection, hidden fault instability interpretation and nonlinear earthquake stability monitoring.

RECOMMENDATION

Future studies should investigate real seismic datasets to validate the proposed synchronisation framework under practical geophysical conditions. Further research should also optimise the neural hyperchaotic subsystem to obtain bounded graphical outputs and improve adaptive seismic signal interpretation. Hardware implementation, real-time monitoring and integration with machine-learning-based seismic classification methods are also recommended.

REFERENCES

Baleanu, D., Diethelm, K., Scalas, E., & Trujillo, J. J. (2012). *Fractional calculus: Models and numerical methods*. World Scientific. https://doi.org/10.1142/8180

Bao, H., Liu, W., Hu, A., & Bao, B. (2021). Memristor-based chaotic systems and their applications. *Nonlinear Dynamics, 103*, 1125–1150. https://doi.org/10.1007/s11071-020-06146-5

Bergen, K. J., Johnson, P. A., de Hoop, M. V., & Beroza, G. C. (2019). Machine learning for data-driven discovery in solid Earth geoscience. *Science, 363*(6433), eaau0323. https://doi.org/10.1126/science.aau0323

Bhat, S. P., & Bernstein, D. S. (2000). Finite-time stability of continuous autonomous systems. *SIAM Journal on Control and Optimization, 38*(3), 751–766. https://doi.org/10.1137/S0363012997321358

Chen, Y., Yang, X., & Li, C. (2022). Finite-time synchronisation of fractionalorder nonlinear systems with uncertain parameters. *Mathematics, 10*(15), 2737. https://doi.org/10.3390/math10152737

Chua, L. O. (1971). Memristor: The missing circuit element. *IEEE Transactions on Circuit Theory, 18*(5), 507–519. https://doi.org/10.1109/TCT.1971.1083337

De Santis, A., Cianchini, G., Favali, P., Beranzoli, L., & Boschi, E. (2019). The earthquake precursors debate. *Annals of Geophysics, 62*(1), SE101. https://doi.org/10.4401/ag-8024

Diethelm, K., Ford, N. J., & Freed, A. D. (2002). A predictor-corrector approach for the numerical solution of fractional differential equations. *Nonlinear Dynamics, 29*, 3–22. https://doi.org/10.1023/A:1016592219341

Dudkowski, D., Jafari, S., Kapitaniak, T., Kuznetsov, N. V., Leonov, G. A., & Prasad, A. Hidden attractors in dynamical systems. *Physics Reports, 637*, 1–50. https://doi.org/10.1016/j.physrep.2016.05.002

Garrappa, R. (2018). Numerical solution of fractional differential equations: A survey and a software tutorial. *Mathematics, 6*(2), 16. https://doi.org/10.3390/math6020016

Geller, R. J., Jackson, D. D., Kagan, Y. Y., & Mulargia, F. (1997). Earthquakes cannot be predicted. *Science, 275*(5306), 1616–1617. https://doi.org/10.1126/science.275.5306.1616

Leonov, G. A., & Kuznetsov, N. V. (2013). Hidden attractors in dynamical systems. *International Journal of Bifurcation and Chaos, 23*(1), 1330002. https://doi.org/10.1142/S0218127413300024

Lorenz, E. N. (1963). Deterministic nonperiodic flow. *Journal of the Atmospheric Sciences, 20*(2), 130–141. https://doi.org/10.1175/1520-0469

Mousavi, S. M., & Beroza, G. C. (2022). Deep-learning seismology. *Science, 377*(6607) eabm4470. https://doi.org/10.1126/science.abm4470

Ngari, A. Z., Ngadda, Y. H., Jauro, D., Teru, P. B., Matthew, A., Dawud, A. M. Chagok, N. M. D (2025) Application of New Mass-Energy Concept in Computation of Q - Values of Nuclear Fission and Fusion Reactions. *Nigerian Journal of Physics (NJP),* 34(1), 96-101. https://doi.org/10.62292/njp.v34i1.2025.387

Pecora, L. M., & Carroll, T. L. (1990). Synchronisation in chaotic systems. *Physical Review Letters, 64*(8), 821–824. https://doi.org/10.1103/PhysRevLett.64.821

Petra´s,ˇ I. (2011). *Fractional-order nonlinear systems: Modelling, analysis and simulation*. Springer. https://doi.org/10.1007/978-3-642-18101-6

Podlubny, I. (1999). *Fractional differential equations*. Academic Press.Scholz, C. H. (2019). *The mechanics of earthquakes and faulting* (3rd ed.). Cambridge University Press. https://doi.org/10.1017/9781316681473

Turcotte, D. L. (2002). *Fractals and chaos in geology and geophysics* (2nd ed.). Cambridge University Press. https://doi.org/10.1017/CBO9781139174695

Yu, F., Zhang, Z., Shen, H., Huang, Y., & Cai, S. (2024). A five-dimensional fractional-order memristive hyperchaotic system with complex dynamics. *Fractal and Fractional, 8*(5), 271. https://doi.org/10.3390/fractalfract8050271